Photometric reduction of images of NGC 3201 stars and inference of their distance and age

M. Funcich, E. Neumerzhitckii

June 14, 2020

Abstract

We present photometric measurements of stars in the direction of the halo globular cluster NGC 3201 in the B, V, R and I bands. Fluxes of stars were measured in each band and converted to magnitudes using photometric calibration equations. By plotting magnitude against colour index we produced a HR diagram of the cluster. Our results compared to SIMBAD proposed a 0.1 and 0.2 mag systematic offset in B and $B-V$ values respectively. Fitting Girardi isochrones using a fixed metallicity of $[Fe/H] = -1.56$ and an applied reddening of $E(B-V) = 0.16$ inferred an age of 13 ± 1 Gyr and a heliocentric distance of 5.5 ± 0.2 kpc to the cluster. Direct calculations for distance propose a lower bound of 1.0 ± 0.4 kpc which agrees with our previous result. Our findings support previous results despite the fact that our data set was missing the main sequence stars. Using age-mass relation of an upper limit main sequence turn-off point suggest an agreed mean upper bound age of 13.6 ± 0.4 Gyr.

1 Introduction

Harbouring the oldest stars in the universe, characterised by their low metallicity and spherical appearance, Globular clusters (GC) aid us into understanding the formation of the Milky Way as well as estimating the lower bound age of the universe. These clusters contain up to millions of stars that are packed closely together due to the strong bounding of their gravity (Chaboyer et al., 1996). The nearby GC NGC 3201 is a prime candidate for age estimation of the

universe as it contains stars that are of same chemical composition as well as age, thus providing a strong age-mass relation (Layden and Sarajedini, 2003; Chaboyer, 1994).

An HR diagram is used to plot the population of stars in a cluster. By plotting the apparent magnitude against colour, we can illustrate several basic features of a globular cluster. These include the evolutionary sequences such as main sequence (MS), the main sequence turnoff (MSTO), the red giant branch (RGB), the asymptotic giant branch (AGB), blue stragglers (BS) as well as RR Lyraes (Ashman and Zepf, 2008). An example of a HR diagram for NGC 3201 is given by Layden and Sarajedini (2003). Incidentally, the locations of the stars on an HR diagram are determined by their mass since the stars in a GC have roughly the same chemical composition and age (Chaboyer, 2001). Accordingly, most of the stars are present in the MS, whereas slightly higher mass stars exhaust their supply of hydrogen in the core and end up in the MSTO. In addition, a defining feature of GC is that the MSTO point occurs at fainter luminosities (Harris and Racine, 1979). For these reasons, the MSTO is a stronger function of age compared to stars on the RGB (Chaboyer, 1994; Sandage, 1970).

The colour index is expressed as the difference between two colours (wavelengths) where the zero-point colour index represents Vega. Cooler stars will have a positive colour index whereas hotter stars will be negative, therefore the HR diagram show the general temperature of the cluster (Alcaino et al., 1989). For our cluster, we use the colour indices B – V, V – R, V – I, B - I and B – R.

In this report, we determine the age and distance of NGC 3201 by fitting theoretical isochrones onto HR diagrams. To improve these stellar models, we account for the cluster's reddening, metallicity and age. Therefore, the age of the GC is the age of the isochrone that best fits the data on the HR diagram (Chaboyer et al., 1996).

2 Method

2.1 Data reduction

The data was taken using an eleven inch aperture telescope located in Monash. The images used in this study are shown in Table 1. We did not make the

observations, the data was given to us in the form of FITS files. We performed bias, dark and flat-field corrections, and then shifted and combined individual science images[1].

Table 1: Images used in this study.

Type	Filter	Number	Exposure [s]	Date
Bias		27	0	13/3/2018
Dark		20	600	15/3/2018
Flat	I, B, V, R	5	4	09/3/2018
Photometric	B	1	30	29/3/2018
Photometric	I, R, V	2	30	29/3/2018
Science	B	16	60	09/3/2018
Science	I	20	60	09/3/2018
Science	R	18	60	09/3/2018
Science	V	17	60	09/3/2018

2.2 Measuring magnitudes of reference stars

We manually selected five bright blue reference stars. Next, we measured the fluxes of the reference stars in our photometric images and calculated their apparent magnitudes using the following calibration equations:

$$\begin{aligned} B &= 19.237 - 2.5\log_{10}(f/t) - 0.330\,A \\ V &= 19.696 - 2.5\log_{10}(f/t) - 0.210\,A \\ R &= 19.679 - 2.5\log_{10}(f/t) - 0.119\,A \\ I &= 19.079 - 2.5\log_{10}(f/t) - 0.134\,A. \end{aligned} \tag{1}$$

Here A is the average airmass number of stacked images, f is the star's flux we measure in the image, in ADU, t is exposure time of the frame, in seconds.

2.3 Measuring magnitudes of all stars

Next, we used the magnitudes of the five reference stars to measure the magnitudes of the rest of the stars in science images using the following equation:

[1]Complete code of this study is available at https://github.com/evgenyneu/asp3231_project. It can be used to reproduce our method, analysis and make the plots shown in this article.

$$m_1 = m_2 - 2.5 \log_{10}(f_1/f_2), \tag{2}$$

where m_1 is the apparent magnitude of a star we want, m_2 is the magnitude of a reference star we calculated previously, f_1 is flux of the star we want, and f_2 is the flux of a reference star. Both f_1 and f_2 fluxes were measured in the same non-photometric image. Using Equation 2 we calculated the magnitude of each individual star five times, using f_2 and m_2 numbers from our five reference stars. The magnitude we used in analysis is the median of these five measurements.

2.4 Estimating magnitude uncertainties

We calculated standard deviation of twenty background fluxes and used it as an estimate of the flux uncertainty $u(f)$ from a star. The uncertainty of reference star magnitude $u(m_2)$ from Equation 1 was propagated using first order approximation

$$u(m_2) = \sqrt{\left[\frac{2.5}{f}\frac{1}{\ln(10)}u(f)\right]^2 + [a\,u(A)]^2},$$

where a is an airmass constant from Equation 1, and $u(A)$ is standard deviation of air mass indices of the stacked images. The uncertainty $u(m_1)$ of magnitudes m_1 from Equation 2 was then propagated using equation

$$u(m_1) = \sqrt{[u(m_2)]^2 + \left[2.5\frac{u(f)}{\ln(10)}\right]^2 \left(\frac{1}{f_1^2} + \frac{1}{f_2^2}\right)},$$

where $u(f)$ is the uncertainty of flux measurement in non-photometric image.

3 Results and analysis

3.1 Colour magnitude diagram

The magnitudes and the colors of the stars that we measured are shown on Figure 1. We can see horizontal and RGB/AGB stars, but main sequence stars were too faint to be measured.

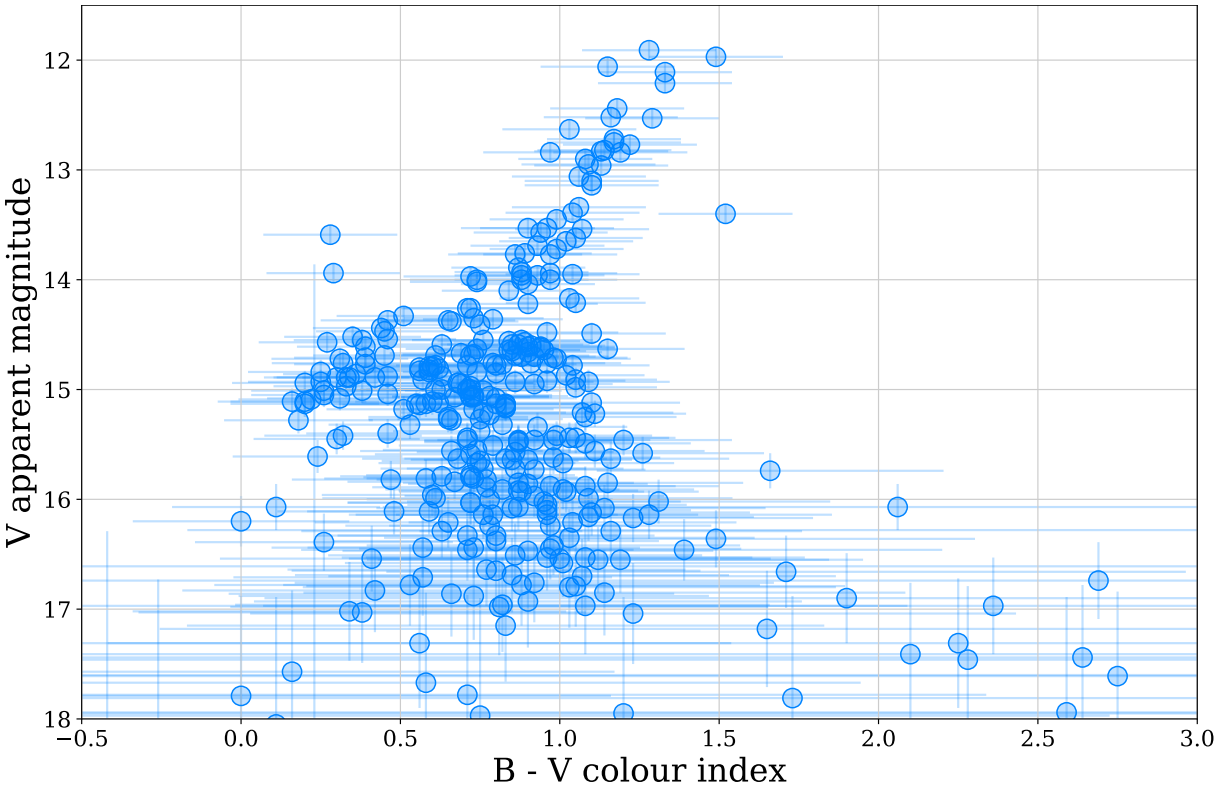

Figure 1: Magnitudes and colors of stars we measured. The error bars are likely to be wrong.

3.2 Comparing our magnitudes with SIMBAD

In order to verify our measurements we compared our B and V magnitudes with SIMBAD database (Wenger et al., 2000). For this comparison we manually selected 25 stars of different magnitudes in the range from 14 to 17 B magnitude. The box plots of the differences between SIMBAD's and our measurements are shown on Figure 2. We can see that our B magnitudes are on average about 0.1 mag smaller than SIMBAD's, and our $B - V$ colours are 0.2 mag smaller. We have verified that this difference is statistically significant using paired sample t-test, with p-value = 0.005 for B values and p-value ≈ 0 for B-V values. Hence, our data suggest that we measured brighter (through B filter) and bluer stars than those reported in SIMBAD.

3.3 Light extinction and reddening

For each of our filters $\lambda = \{B, V, R, I\}$ we calculated extinction values A_λ, shown in Table 2, using equation

$$A_\lambda = R_V \, E(B - V) \, \frac{A_\lambda}{A_V},$$

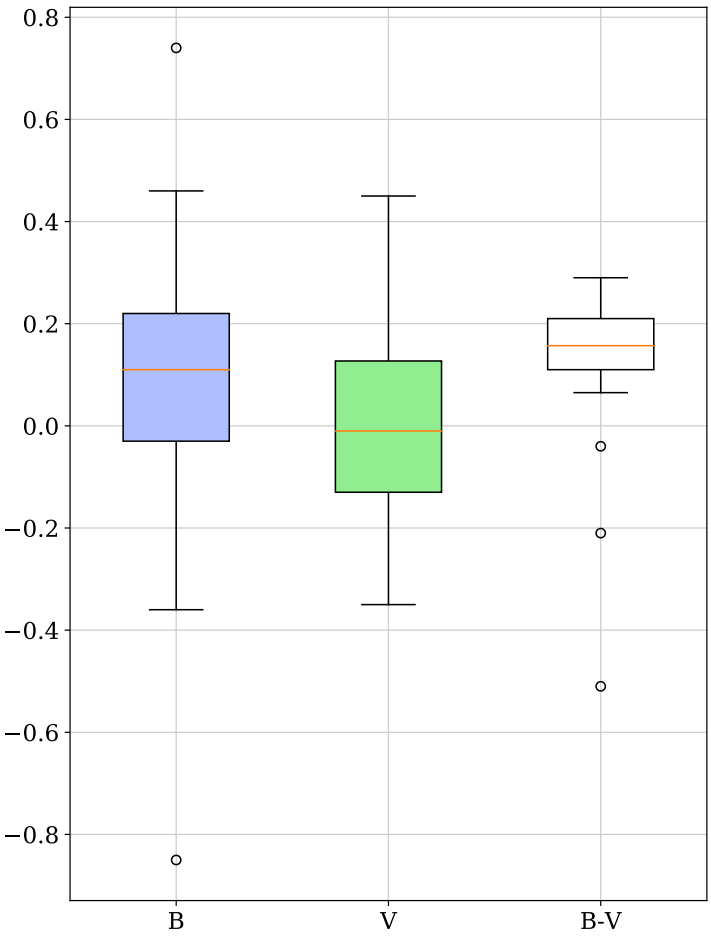

Figure 2: Summary of magnitude differences for 25 stars: SIMBAD minus this study. There could be 0.1 and 0.2 mag systematic offsets in B and $B-V$ values respectively.

where $R_V = 3.1$ is total-to-selective extinction ratio from Cardelli et al. (1989), $E(B-V) = 0.14$ is reddening from Alcaino (1976), and A_λ/A_V is the extinction ratio from table A4 in Gordon et al. (2003) for Small Magellanic Cloud.

Table 2: Extinction values for the filters.

Filter	**Extinction A_λ [mag]**
B	0.59
V	0.43
R	0.35
I	0.25

Next, we used extinction values A from Table 2 to calculate reddening

numbers $E(X-Y)$ using the definition of reddening:

$$E(X-Y) = A_X - A_Y, \tag{3}$$

where X and Y are filter names $X, Y = \{B, V, R, I\}$.

3.4 Girardi isochrone fitting

One method of estimating the age and distance is to fit theoretical isochrones to our data. The isochrones we used for fitting were generated using an interactive web interface[2] which included parameters of age and metallicity. To get an approximate age we plotted isochrones from ages 10 to 16 Gyrs. Since we did not measure MSTO stars we relied on matching the RGB, AGB and HB instead.

Firstly, we adopted metallicity values from literature, where Gonzalez and Wallerstein (1998) calculated $[Fe/H] = -1.42 \pm 0.03$ using spectroscopy and photometry from the echelle spectra of 18 giants whereas Kraft and Ivans (2003) claimed $[Fe/H] = -1.56$ using spectroscopy and utilised the Fe II line. Generating these isochrones, we found that Kraft and Ivans (2003) gave the best shape along the AGB and HB. Using a higher metallicity value caused stars on the AGB to have luminosities greater than our data. Additionally, we applied reddening to our isochrones to compensate for the dust extinction causing NGC 3201 to appear fainter, where $E(B-V) = 0.16$, computed using Equation 3.

When fitting reddened isochrones to our data we estimated the true apparent distance modulus $(m-M)_0$. This was done by shifting the isochrones in the V magnitude until it matched the cluster's evolutionary tracks, the amount of shift is then equal to $(m-M)_0$ mag. This process could result in systematic errors as it's done by roughly estimating the best fit, thus we plotted an upper and lower limit of $(m-M)_0$ to estimate an uncertainty.

The fitted reddened isochrones were generated with $[Fe/H] = -1.56$, $E(B-V) = 0.16$ and ages 12, 13, 14 Gyrs, thus estimating a $(m-M)_0$ of 13.69 ± 0.1 mags as shown in Figure 3. To calculate the distance we used the following equation

$$(m-M)_0 = 5\log_{10}\left(\frac{d}{10pc}\right) \tag{4}$$

[2] http://stev.oapd.inaf.it/cgi-bin/cmd

giving us a distance of 5.5 ± 0.2 kpc and an age of 13 ± 1 Gyrs for NGC 3201.

Using values from literature we compare how reddening influences our isochrones and results. We estimated the distance of NGC 3201 to be 4.2 kpc using $E(B-V) = 0.25$ (Monty et al. (2018)) and 5.3 kpc using $E(B-V) = 0.14$ (Alcaino (1976)). Through observational analysis of the fit, our value for $E(B-V) = 0.16$ provided the best shape for our isochrones.

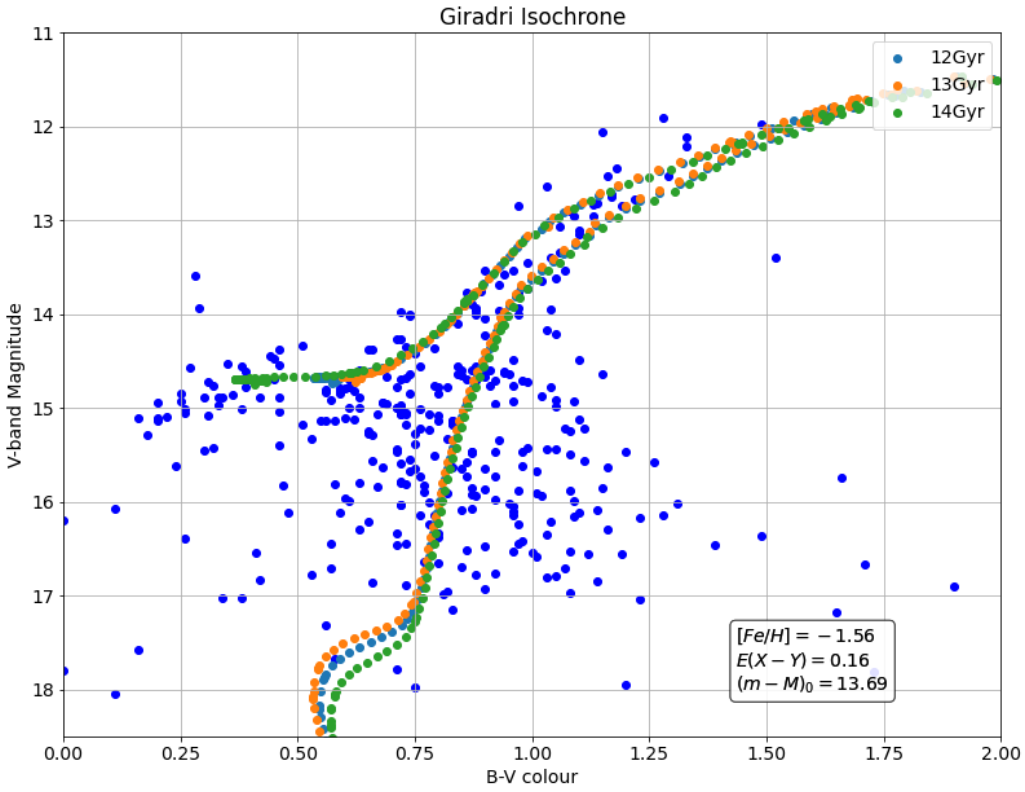

Figure 3: HR Diagram of NGC 3201 with fitted reddened isochrones with metallicity [Fe/H] = -1.56, shifted by a distance modulus of $(m-M)_0 = 13.69$ mag. Ages of isochrones are 12, 13 and 14 Gyr.

3.5 Using MSTO to estimate age and distance

An alternative method we used to find age and distance was to use data provided by Carroll and Ostlie (2007). First, we removed the reddening from NGC 3201 using $E(B-V) = 0.16$ value. Since MSTO was absent, using the fact that the relative bluer red giant stars are redder than the MSTO, we estimated a rough upper limit of $0.70 \leq (B-V) \leq 0.73$, which corresponds to an apparent magnitude range of $13 \leq m_V \leq 16$.

Next, we plotted $(B-V)$ colour against absolute magnitude M_V using data from the Appendix: Stellar Data, Main-sequence stars (Luminosity Class V) table provided by Carroll and Ostlie (2007). Using the line of best fit we determined that $5.3 \leq M_V \leq 5.5$ using our range for $(B-V)$. Rearranging and substituting our values into equation

$$m_V - M_V = 5 \log_{10} \left(\frac{d}{10pc} \right) \tag{5}$$

we get a lower limit of the distance $d > 1.0 \pm 0.4$ kpc.

To calculate age we used the relation that age is proportional to $M^{-2.5}$, where M is the mass of a star in solar masses. Similarly to the distance method, we plotted mass against $(B-V)$ colour using data from the Carroll and Ostlie (2007) appendix table. From our $(B-V)$ colour limit, we obtained a $M_\odot \leq 0.9$. Using the relation mentioned, we estimate the mean upper limit of age to be 13.6 ± 0.4 Gyr.

3.6 HR diagram in BVRI colours

In Figure 4, we plot several different HR diagrams and fit isochrones to them. We then apply the method in section 3.4 to estimate distance and age. Table 3 summarises the results, where reddening is calculated using the extinction values in Table 2.

Table 3: Reddening, distance and age of NGC 3201 using various colour indices.

Colour	Reddening	Distance [kpc]	Age [Gyr]
B - V	0.16	5.5	13 ± 1
B - R	0.24	5.0	14 ± 1
B - I	0.34	4.6	14 ± 1
V - R	0.08	6.0	15 ± 1
V - I	0.18	6.6	13 ± 1

We evidently see in Figure 4 that both B - R and B - I are spread out and show a strong correlation in HB. The RGB is most prominent and denser in the V - I and V - R band. However, the reddening calculated for V - I is is not alligned, thus appearing bluer compared to the data, therefore the age and distance is highly uncertain for this colour. Our results infer that using different colour influences age, in this case by 1 to 2 Gyrs compared to the B - V colour index.

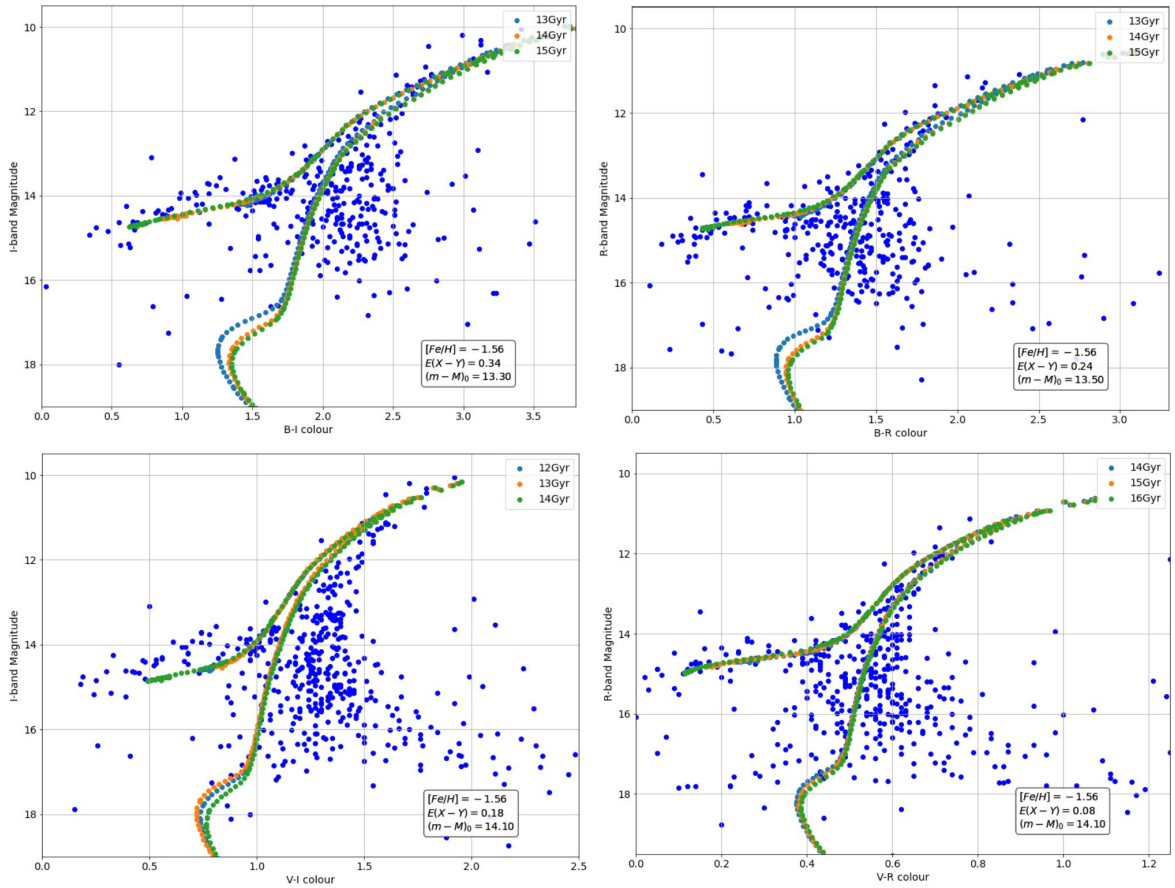

Figure 4: HR diagrams of the same stars using different colour indices. From left to right: m_I against B - I, m_R against B - R, m_I against V - I, and m_R against V - R

4 Discussion

The error of estimating the distance and age of the GC NGC 3201 was hindered by the methodology of deriving data from the MSTO point. Our investigation faced drawbacks from the performance of the telescope as it was unable to detect MS stars. Consequently, no MSTO point was identified on our HR diagrams. Using only the RGB, AGB and HB for fitting isochrones results in less precise age measurements than MSTO. This is evident in Figure 3, where the RGB and AGB don't differ with age compared to the MSTO. In a future study, it is recommended we redo the photometry using a telescope with a larger aperture. This would allow us to collect a larger sample of photons from fainter stars, which in turn would help identify the MSTO for the cluster.

4.1 Limitations of Girardi isochrones

Our results derived using models of isochrones are tabulated in Table 3 for a variety of colours. The assumed metallicity, reddening and distance modulus became our primary sources of uncertainty for modelling our GC.

Metallicity values from literature inferred that our cluster was metal-poor, we confirmed this was true by generating isochrones using $[Fe/H]$ values adopted from Kraft and Ivans (2003) and Gonzalez and Wallerstein (1998). This in turn, suggests our isochrones are relatively good models for our data. To improve the accuracy of our assumption, we chose the value that gave the best model. However, this still embeds an unknown value for uncertainty. Therefore, to get an accurate representation of the stellar evolution for our data, we could have performed our own spectroscopy, thus determining our own metal abundance ratio $[Fe/H]$.

To increase the accuracy of our models, we tested various reddening values. Our results compared to literature showed that our E(B - V) was bluer than Monty et al. (2018) and slightly redder than Alcaino (1976). Our value compared to literature was best for correcting the interference of dust. The uncertainty of reddening and extinction is discussed further in depth later in the discussion.

Lastly, the distance modulus calculated relied on the above factors to be accurate, as well as presence of a turn-off point. Since the latter was missing, we took a mean value for $(m - M)_0$ to estimate the uncertainty of distance modulus. Hence our uncertainty was ± 0.1. McNamara (1997) applies a sophisticated approach for calculating uncertainty, where they investigate the pulsation of variable stars (period - luminosity relation) to calibrate the distance modulus of the Magellanic cloud. Further studies (Layden and Sarajedini, 2003; Harris and Racine, 1979) implement this technique to calculate $(m - M)_0$ of NGC 3201.

4.2 Age

Basing age off our isochrone models in (B - V) colour index suggests only a broad representation of NGC 3201's age. A study that agreed with our results was by Layden and Sarajedini (2003) who also calculated a large uncertainty when fitting models to the MSTO, thus determining an age of $\approx 13 \pm 2$ Gyr. Alternative studies suggest a lower age of 12.2 ± 0.5 Gyr and 12.00 ± 0.75 Gyr

(Monty et al., 2018; Dotter et al., 2009). Our estimation could have been improved if we were able to fit along the MS which would have allowed us to narrow the age range of our isochrones.

The upper age limit calculated using age-mass relation agreed with literature. However, since we relied on (B - V) colour to estimate age, the systematic error of our magnitudes could have influenced our estimates. This discrepancy is mentioned in more detail in section 4.7.

Our findings suggest that our cluster is close to the age of the universe as proposed by Bolte and Hogan (1995); Chaboyer et al. (1996); Freedman (2000). Thus the lower age limit of our universe is $\approx$ 12 to 14 Gyrs old. However, it is clear that our assumption is biased as it is based off one cluster. Further studies as presented by Chaboyer et al. (1996) determined the ages of 17 GCs and plotted them on a probability distribution curve which they determined a 95 percent confidence limit lower bound occurring at age 12.07 Gyr, and the median age of 14.56 Gyr years.

4.3 Distance

Our estimation for B - V distance using Equation 4 agreed with literature. Alcaino (1976) and Monty et al. (2018) determined a distance of 5.4 and 5.1 $\pm$ 0.1 kpc, respectively. However, the distance we calculated using data from Carroll and Ostlie (2007) was a lower bound distance, which is $\approx$ 4 kpc lower than the value from literature. This discrepancy is likely caused due to the crude approximation of the upper estimate of $0.70 \leq (B-V) \leq 0.73$ for MSTO stars. Again, it would be best if we had data from the turn-off point.

4.4 Colour indices

In addition to B-V, we used other colors for Girardi fits. In particular, the B-I color is a larger color range than B-V, and therefore B-I spreads out the blue markers more horizontally (top left sub-plot on Figure 4). This makes it easier for us to see the red and horizontal branches and, thus easier to fit the isochrones.

4.5 Uncertainties

We calculated magnitude uncertainties (section 2.4) by measuring the standard deviation of fluxes in star-free regions and assuming that it is equal to

flux uncertainty in the regions with stars. This method almost certainly gives wrong uncertainties, since regions with stars collect more photons, and therefore there should be additional uncertainty due to photon arrival, modelled by Poisson probability distribution. A correct way of calculating magnitude uncertainty would be to estimate the flux variance for each individual pixel of the raw image and then propagate the variance through all the image reduction steps.

4.6 Light extinction and reddening

We calculated light extinction (section 3.3) based on measurements extinction ratios A_λ/A_V from Gordon et al. (2003). These measurements were made for Small Magellanic Cloud, and not for NGC 3201. Therefore, our reddening and extinction values could have systematic errors, which would bias our estimates of distance and age. Moreover, we used a single value of reddening for each color for all observed stars. However, reddening E(B-V) varies by 0.2 mag across NGC 3201 (von Braun and Mateo, 2001). Therefore, it would be better to use a 2D map of reddening and apply it to correct magnitudes for each individual stars.

4.7 Systematic error in B-V color

We have found a statistically significant shift of 0.2 mag in B-V color when compared with SIMBAD database (section 3.2). If we assume that SIMBAD's measurements are accurate, then our measurements should be shifted by 0.2 mag to the right on Figure 3, which will affect the isochrone fits and will lead to a higher age estimate.

We can see two possible causes of this shift in the E-B color. Firstly, the shift could be caused by inaccurate photometric calibration (Equation 1). Secondly, we have used only one frame from the B-band photometric night (Table 1) to calculate the magnitude of the B magnitude of the reference stars (section 2.2). This resulted in low signal-to-noise and could cause inaccurate measurements. Thus, in order to fix the color shift issue, we would recommend repeating the photometric calibration and taking more photometric images.

5 Conclusion

We have presented photometric observations of the GC NGC 3201. We interpreted the data and estimated the age of the cluster in $(B-V)$ to be 13 ± 1 Gyrs from Girardi isochrones and a mean upper bound of 13.6 ± 0.4 Gyr from age-mass relations. From the isochrones we estimate a distance of 5.5 ± 0.2 kpc to the cluster. This is agrees with the upper limit turn-off point, where applying our values to the distance modulus formula we estimate a mean lower bound distance of $d > 1.0 \pm 0.4$ kpc. Due to the limitations of our data set, our results could easily be improved by using a bigger telescope. From our investigation of this GC we infer a lower age limit of our universe to be, approximately, between 12 and 14 Gyrs old.

References

Alcaino, G. (1976). The globular cluster ngc 3201. *Astronomy and Astrophysics Supplement Series*, 26:251–259.

Alcaino, G., Liller, W., and Alvarado, F. (1989). Bvri ccd photometry of the globular cluster ngc 3201. *Astronomy and Astrophysics*, 216:68–79.

Ashman, K. M. and Zepf, S. E. (2008). *Globular cluster systems*, volume 30. Cambridge University Press.

Bolte, M. and Hogan, C. J. (1995). Conflict over the age of the universe. *Nature*, 376(6539):399–402.

Cardelli, J. A., Clayton, G. C., and Mathis, J. S. (1989). The Relationship between Infrared, Optical, and Ultraviolet Extinction. ApJ, 345:245.

Carroll, B. W. and Ostlie, D. A. (2007). *An Introduction to Modern Astrophysics*. 2nd (international) edition.

Chaboyer, B. (1994). Absolute ages of globular clusters and the age of the universe. *arXiv preprint astro-ph/9412015*.

Chaboyer, B. (2001). Globular cluster age dating. In *Astrophysical Ages and Times Scales*, volume 245, page 162.

Chaboyer, B., Demarque, P., Kernan, P. J., and Krauss, L. M. (1996). A lower limit on the age of the universe. *Science*, 271(5251):957–961.

Dotter, A., Sarajedini, A., Anderson, J., Aparicio, A., Bedin, L. R., Chaboyer, B., Majewski, S., Marín-Franch, A., Milone, A., Paust, N., et al. (2009). The acs survey of galactic globular clusters. ix. horizontal branch morphology and the second parameter phenomenon. *The Astrophysical Journal*, 708(1):698.

Freedman, W. L. (2000). The hubble constant and the expansion age of the universe. *Physics Reports*, 333:13–31.

Gonzalez, G. and Wallerstein, G. (1998). Elemental abundances in giants in ngc 3201, a globular cluster with a retrograde orbit. *The Astronomical Journal*, 116(2):765.

Gordon, K. D., Clayton, G. C., Misselt, K. A., Land olt, A. U., and Wolff, M. J. (2003). A Quantitative Comparison of the Small Magellanic Cloud, Large Magellanic Cloud, and Milky Way Ultraviolet to Near-Infrared Extinction Curves. ApJ, 594(1):279–293.

Harris, W. E. and Racine, R. (1979). Globular clusters in galaxies. *Annual Review of Astronomy and Astrophysics*, 17(1):241–274.

Kraft, R. P. and Ivans, I. I. (2003). A globular cluster metallicity scale based on the abundance of feii. *Publications of the Astronomical Society of the Pacific*, 115(804):143.

Layden, A. C. and Sarajedini, A. (2003). Photometry of the globular cluster ngc 3201 and its variable stars. *The Astronomical Journal*, 125(1):208.

McNamara, D. (1997). Luminosities of sx phoenicis, large-amplitude delta scuti, and rr lyrae stars. *Publications of the Astronomical Society of the Pacific*, 109(741):1221.

Monty, S., Puzia, T. H., Miller, B. W., Carrasco, E. R., Simunovic, M., Schirmer, M., Stetson, P. B., Cassisi, S., Venn, K. A., Dotter, A., et al. (2018). The gems/gsaoi galactic globular cluster survey (g4cs). i. a pilot study of the stellar populations in ngc 2298 and ngc 3201. *The Astrophysical Journal*, 865(2):160.

Sandage, A. (1970). Main-sequence photometry, color-magnitude diagrams, and ages for the globular clusters m3, m13, m15, and m92. *The Astrophysical Journal*, 162:841.

von Braun, K. and Mateo, M. (2001). An extinction map and color-magnitude diagram for the globular cluster NGC 3201. *The Astronomical Journal*, 121(3):1522–1532.

Wenger, M., Ochsenbein, F., Egret, D., Dubois, P., Bonnarel, F., Borde, S., Genova, F., Jasniewicz, G., Laloë, S., Lesteven, S., and Monier, R. (2000). The SIMBAD astronomical database. The CDS reference database for astronomical objects. A&AS, 143:9–22.